FRACTIONAL-STEP METHODS AND FINITE ELEMENTS WITH SYMMETRIC STABILIZATION FOR THE TRANSIENT OSEEN PROBLEM

Erik Burman[1], Alexandre Ern[2] and Miguel A. Fernández[3,4]

Abstract. This paper deals with the spatial and time discretization of the transient Oseen equations. Finite elements with symmetric stabilization in space are combined with several time-stepping schemes (monolithic and fractional-step). Quasi-optimal (in space) and optimal (in time) error estimates are established for smooth solutions in all flow regimes. We first analyze monolithic time discretizations using the Backward Differentiation Formulas of order 1 and 2 (BDF1 and BDF2). We derive a new estimate on the time-average of the pressure error featuring the same robustness with respect to the Reynolds number as the velocity estimate. Then, we analyze fractional-step pressure-projection methods using BDF1. The stabilization of velocities and pressures can be treated either implicitly or explicitly. Numerical results illustrate the main theoretical findings.

Mathematics Subject Classification. 65M12, 65M60, 76D07, 76M10.

1. Introduction

The computation of Navier–Stokes flows at high Reynolds number is an important challenge in scientific computation. Many space discretization methods rely crucially on the presence of non-negligible viscous dissipation and therefore lack robustness when the mesh Reynolds number $\frac{|\beta| h}{\mu}$ (β is the flow velocity, h the mesh size, and μ the viscosity parameter) is much larger than one. In this regime, the standard Galerkin formulation is known to be unstable even in the linear case, and these instabilities tend to be amplified by nonlinearities. To counter such instabilities, one may resort to stabilization techniques, such as SUPG [23], discontinuous Galerkin [13, 22], or H^1-conforming finite elements with symmetric stabilization in various flavors [1, 6, 9, 17]. The effect of stabilization is on the one hand to improve the convergence to smooth solutions. On the other hand, for rough solutions, stabilization limits the propagation of perturbations generated in the vicinity of sharp gradients; stabilization also turns out to promote the Gibbs phenomenon when approximating rough solutions to conservation laws, and this effect can be tempered by some nonlinear weighting mechanism [14].

[1] Department of Mathematics, University College London, Gower Street, London, WC1E 6BT, UK. E.Burman@ucl.ac.uk

[2] Université Paris-Est, CERMICS (ENPC), 77455 Marne la Vallée cedex 2, France. alexandre.ern@enpc.fr

[3] Inria, 75012 Paris, France. miguel.fernandez@inria.fr

[4] Sorbonnes Universités, UPMC, Laboratoire Jacques-Louis Lions, 75005 Paris, France.

In this paper, we are interested in combining stabilized finite elements for space discretization with time discretization schemes for fluid flow problems in the high Reynolds number regime. The importance of stabilization in the high Reynolds number regime for fractional-step methods was illustrated numerically in [19] for Navier–Stokes flows, showing that the pressure-projection method can fail to converge in the high Reynolds number regime unless some stabilization is applied. Our goal here is to provide some theoretical background analyzing this fact. For simplicity, we focus on the linearized version of the Navier–Stokes equations known as the Oseen equations, and we prove that stabilized finite element methods also improve the convergence rate to smooth solutions when using a fractional-step pressure-projection scheme for time discretization. Let Ω be a bounded polyhedron in $\mathbb{R}^d$, $d \in \{2,3\}$, with boundary $\partial\Omega$ and outward pointing normal ν, and let t_{F} be a finite positive time. We consider the Oseen equations posed in the space-time cylinder $Q := \Omega \times (0, t_{\mathrm{F}})$,

$$\partial_t u + \beta\cdot\nabla u - \mu\Delta u + \nabla p = f, \tag{1.1a}$$
$$\nabla\cdot u = 0, \tag{1.1b}$$

where the unknowns are the velocity field u and the pressure p, while the data are the advection velocity β, the viscosity μ, and the body force f. We assume that the velocity field β is Lipschitz (with Lipschitz constant denoted by L_β) and divergence-free, that μ is a positive real number, and that $f \in L^2(0, t_{\mathrm{F}}; L^2(\Omega)^d)$. The Oseen equations are supplemented with a homogeneous Dirichlet boundary condition on the velocity and an initial condition on the velocity of the form $u|_{t=0} = u_0$, with $u_0 \in H_0^1(\Omega)^d$ and $\nabla\cdot u_0 = 0$.

The quasi-optimal approximation of smooth solutions to the stationary Oseen equations using finite elements with symmetric stabilization in various flavors has been investigated in [2]. In the unstationary case, the literature on projection methods for the Navier–Stokes equations is very rich, starting with the pioneering work by Chorin and Temam, Yosida and more recent work (see, *e.g.*, [10, 20, 26] and references therein). Nevertheless, a complete analysis including space discretization using stabilized finite elements is, to our knowledge, not yet available, even in the linearized case of the unstationary Oseen equations. In the present work, we provide such an analysis. We focus on stabilization using the continuous interior penalty finite element method analyzed in [7] for the stationary Oseen equations. The stabilization concerns the advective derivative and the pressure-velocity coupling, whereas a least-squares penalty on the velocity divergence is also considered. Moreover, the homogeneous Dirichlet boundary condition on the velocity is enforced weakly using the classical boundary penalty method of Nitsche [25]. It is straightforward to extend the present results to other methods using symmetric stabilization such as interior penalty discontinuous Galerkin methods [11, 12, 15], or the orthogonal subscales method [9]. Nonsymmetric stabilized methods like SUPG on the other hand do not fit the proposed analysis framework and remain a topic for future work.

This paper is organized as follows. In Section 2, we present the discrete setting. In Section 3, we analyze monolithic time discretizations, including both first- and second-order Backward Differentiation (BDF) schemes. The main result is Theorem 3.1. While the velocity estimate follows using standard arguments based on [4], the pressure estimate, inspired by the recent asymptotic analysis of [8], is, to our knowledge, new. The idea is to bound the time-average of the pressure error, so as to achieve the same type of robustness with respect to the Reynolds number as for the velocity estimate. Note that stabilization plays a role in achieving this result. In Section 4, we analyze the fractional-step time discretization using pressure-projection, focusing on the first-order BDF scheme. The main result is Theorem 4.7 providing (quasi-optimal in space and optimal in time) error estimates that are independent of the viscosity (but not of high-order Sobolev norms of the exact solution). Moreover, Corollary 4.2 shows that it is possible to treat velocity and/or pressure stabilization either implicitly or explicitly in time, up to some modifications of the CFL condition on the time step. From the point of view of computation, it can be advantageous to treat the stabilization explicitly. In particular, this eliminates the need for the construction of a system matrix with a nonstandard stencil. Finally, in Section 5, we present numerical results illustrating the theoretical analysis.

2. The discrete setting

Let $L := L^2(\Omega)$ and $L_* := \{q \in L;\ \int_\Omega q = 0\}$. For a subset $S \subset \Omega$, we denote by $(\cdot, \cdot)_{L,S}$ and $\|\cdot\|_{L,S}$ respectively the standard inner product and norm of $L^2(S)$, with the convention that the index S is omitted if $S = \Omega$.

2.1. Space semi-discrete Oseen equations

Let $\{\mathcal{T}_h\}_{h>0}$ be a family of affine, simplicial meshes of Ω. We assume that the meshes are kept fixed in time and, for simplicity, the family $\{\mathcal{T}_h\}_{h>0}$ is supposed to be quasi-uniform. Mesh faces are collected in the set $\mathcal{F}_h$ which is split into the set of interior faces, $\mathcal{F}_h^{\mathrm{int}}$, and of boundary faces, $\mathcal{F}_h^{\mathrm{ext}}$. For a smooth enough function v that is possibly double-valued at $F \in \mathcal{F}_h^{\mathrm{int}}$ with $F = \partial T^- \cap \partial T^+$, we define its jump at F as $[\![v]\!] := v|_{T^-} - v|_{T^+}$, and we fix the unit normal vector to F, denoted by ν_F, as pointing from T^- to T^+. The arbitrariness in the sign of $[\![v]\!]$ is irrelevant in what follows.

We consider continuous finite elements with equal-order to discretize in space the velocity and the pressure. Let $k \geq 1$ be an integer and set

$$M_h := \{m_h \in C^0(\overline{\Omega});\ \forall T \in \mathcal{T}_h,\ m_h|_T \in \mathbb{P}_k(T)\}, \tag{2.1}$$

with $\mathbb{P}_k(T)$ spanned by the restriction to T of polynomials of total degree $\leq k$. Set

$$V_h := [M_h]^d, \qquad P_h = M_h \cap L_*, \tag{2.2}$$

and observe that the boundary condition on the velocity is to be enforced weakly. We also need the extended space

$$\widetilde{V}_h := V_h + \nabla P_h. \tag{2.3}$$

To express the divergence-free constraint at the discrete level, we consider the discrete operator $B_h : V_h \to P_h$ such that for all $(v_h, q_h) \in V_h \times P_h$,

$$(B_h v_h, q_h)_L := -(\nabla \cdot v_h, q_h)_L + (\nu \cdot v_h, q_h)_{L,\partial\Omega}, \tag{2.4}$$

and its transpose $B_h^{\mathrm{T}} : P_h \to V_h$. As motivated in [18], we also consider the extension of B_h to $\widetilde{V}_h$, namely $C_h : \widetilde{V}_h \to P_h$ such that for all $(\widetilde{v}_h, q_h) \in \widetilde{V}_h \times P_h$,

$$(C_h \widetilde{v}_h, q_h)_L := (\widetilde{v}_h, \nabla q_h)_L. \tag{2.5}$$

Integration by parts yields $B_h = C_h i_h$ where i_h is the canonical injection of V_h into $\widetilde{V}_h$. Moreover, the transpose $C_h^{\mathrm{T}} : P_h \to \widetilde{V}_h$ is the restriction of the gradient operator to P_h, and we infer that $B_h^{\mathrm{T}} = i_h^{\mathrm{T}} C_h^{\mathrm{T}}$ where i_h^{T} coincides with the (restriction to $\widetilde{V}_h$ of the) L-orthogonal projection onto V_h, henceforth denoted by π_h. To alleviate the notation in what follows, we omit the operator i_h. We extend the domains of B_h, C_h, and their transposes to smooth functions by setting $(B_h v, q_h)_L := -(\nabla \cdot v, q_h)_L + (\nu \cdot v, q_h)_{L,\partial\Omega}$ and $(C_h v, q_h)_L := (v, \nabla q_h)_L$ for all $q_h \in P_h$ and all $v \in [H^1(\Omega)]^d$, and $C_h^{\mathrm{T}} q = \nabla q$ for all $q \in H^1(\Omega)$, while $B_h^{\mathrm{T}} q = i_h^{\mathrm{T}} \nabla q$.

To discretize the convection-diffusion operator in (1.1a), we consider the continuous interior penalty finite element method analyzed in [7] for the stationary Oseen equations. We introduce the discrete operator $A_h : V_h \to V_h$ such that, for all $(v_h, w_h) \in V_h \times V_h$,

$$\begin{aligned}
(A_h v_h, w_h)_L := {}& (\beta \cdot \nabla v_h, w_h)_L + \sum_{F \in \mathcal{F}_h^{\mathrm{ext}}} ((\beta \cdot \nu_F)^\ominus v_h, w_h)_{L,F} \\
&+ (\mu \nabla v_h, \nabla w_h)_L - (\mu(\nu \cdot \nabla v_h), w_h)_{L,\partial\Omega} - (v_h, \mu(\nu \cdot \nabla w_h))_{L,\partial\Omega} \\
&+ \sum_{F \in \mathcal{F}_h^{\mathrm{ext}}} \gamma_1 h_F^{-1} (\mu v_h, w_h)_{L,F},
\end{aligned} \tag{2.6}$$

where for a real number x, $x^\ominus = \frac{1}{2}(|x| - x)$ denotes its negative part ($x^\oplus = \frac{1}{2}(|x| + x)$ denotes its positive part), and where γ_1 is a user-dependent positive parameter related to the boundary penalty method. Furthermore, we consider the stabilization operators $S_h^u : V_h \to V_h$ and $S_h^p : P_h \to P_h$ such that for all $(v_h, w_h) \in V_h \times V_h$ and $(q_h, r_h) \in P_h \times P_h$,

$$(S_h^u v_h, w_h)_L := \sum_{F \in \mathcal{F}_h^{\mathrm{int}}} \gamma_2 \xi_F \beta_{\nu, F} h_F^2 (\llbracket \nu_F \cdot \nabla v_h \rrbracket, \llbracket \nu_F \cdot \nabla w_h \rrbracket)_{L, F}$$

$$+ \sum_{K \in \mathcal{T}_h} \widetilde{\gamma}_3 \max_{F \in \partial K} (\xi_F \beta_F h_F)(\nabla \cdot v_h, \nabla \cdot w_h)_K$$

$$+ \sum_{F \in \mathcal{F}_h^{\mathrm{ext}}} \gamma_3 \beta_F (\nu_F \cdot v_h, \nu_F \cdot w_h)_{L, F}, \tag{2.7a}$$

$$(S_h^p q_h, r_h)_L := \sum_{F \in \mathcal{F}_h^{\mathrm{int}}} \gamma_4 \xi_F \beta_F^{-1} h_F^2 (\llbracket \nabla q_h \rrbracket, \llbracket \nabla r_h \rrbracket)_{L, F}, \tag{2.7b}$$

with local velocities $\beta_{\nu, F} := \|\beta \cdot \nu_F\|_{L^\infty(F)}$ and $\beta_F := \|\beta\|_{[L^\infty(F)]^d}$, user-dependent positive parameters γ_2, $\widetilde{\gamma}_3$, γ_3 and γ_4, and cut-off function $\xi_F = \min(1, \mathrm{Re}_F)$ with local face Reynolds number $\mathrm{Re}_F := \frac{h_F \beta_F}{\mu}$ (note that in (2.7b), $\xi_F \beta_F^{-1}$ is bounded by $\mu^{-1} h_F$ if β vanishes on F). The aim of the stabilization operators is to stabilize the advection operator (sum with γ_2), achieve additional control on the incompressibility condition (sums with $\widetilde{\gamma}_3$ and γ_3), and ensure inf-sup stability for the pressure-velocity coupling (sum with γ_4). The domain of the discrete operators A_h, S_h^u, and S_h^p can be extended to smooth functions by setting $A_h v = \pi_h(\beta \cdot \nabla v - \mu \Delta v)$, $S_h^u v = 0$ for all $v \in [H^2(\Omega) \cap H_0^1(\Omega)]^d$ with $\nabla \cdot v = 0$, and $S_h^p q = 0$ for all $q \in H^2(\Omega)$.

The space semi-discrete Oseen equations take the following form: Find $u_h \in C^1([0, t_{\mathrm{F}}]; V_h)$ and $p_h \in C^0([0, t_{\mathrm{F}}]; P_h)$ such that, for all $t \in (0, t_{\mathrm{F}})$,

$$\partial_t u_h + A_h u_h + S_h^u u_h + B_h^{\mathrm{T}} p_h = f_h \quad (\text{in } V_h), \tag{2.8a}$$

$$-B_h u_h + S_h^p p_h = 0 \quad (\text{in } P_h), \tag{2.8b}$$

where $f_h := \pi_h f$. This problem was analyzed in [4].

2.2. Analysis tools

We consider the following norm on $V_h + [H^2(\Omega)]^d$:

$$\|v\|_{\mu, \beta} := \mu^{\frac{1}{2}}(\|\nabla v\|_L + h^{-\frac{1}{2}} \|v\|_{L, \partial\Omega} + h^{\frac{1}{2}} \|\nu \cdot \nabla v\|_{L, \partial\Omega}) + \| |\beta \cdot \nu|^{\frac{1}{2}} v\|_{L, \partial\Omega}, \tag{2.9}$$

together with the following semi-norms on $V_h + [H^2(\Omega)]^d$ and $P_h + H^2(\Omega)$, respectively,

$$|v|_{S^u} := (S_h^u v, v)_L^{\frac{1}{2}}, \qquad |q|_{S^p} := (S_h^p q, q)_L^{\frac{1}{2}}. \tag{2.10}$$

It is well-known that for γ_1 large enough, using integration by parts and discrete trace inequalities, one can show that $\|\nabla v_h\|_L^2 - 2(\nu \cdot \nabla v_h, v_h)_{L, \partial\Omega} + \sum_{F \in \mathcal{F}_h^{\mathrm{ext}}} \gamma_1 h_F^{-1} \|v_h\|_{L, F}^2 \gtrsim \|\nabla v_h\|_L^2 + h^{-1} \|v_h\|_{L, \partial\Omega}^2$ for all $v_h \in V_h$, so that the following holds:

$$(A_h v_h, v_h)_L \gtrsim \|v_h\|_{\mu, \beta}^2, \qquad \forall v_h \in V_h. \tag{2.11}$$

The above assumption on γ_1 is implicitly made in what follows. Here and in what follows, we abbreviate $A \lesssim B$ the inequality $A \le cB$ for positive real numbers A and B, where the value of c can change at each occurrence while being independent of the mesh size and the physical parameters β, μ and t_{F} (c can depend on the polynomial degree k and the stabilization constants γ_i, $i = 1, \ldots, 4$).

Lemma 2.1 (Boundedness on orthogonal subscales). *Let $v \in V_h + [H^2(\Omega)]^d$ and let $q \in M_h + H^2(\Omega)$. Assume that $(v, w_h)_L = 0$ for all $w_h \in V_h$ and that $(q, r_h)_L = 0$ for all $r_h \in M_h$ (functions satisfying such properties are called orthogonal subscales). Let $c(\beta, h) := \max_{F \in \mathcal{F}_h^{\mathrm{int}}}(\xi_F^{-1}\beta_F)$ and $\check{c}(\beta, h) := \max_{F \in \mathcal{F}_h}(\xi_F \beta_F^{-1})$. Then, for all $q_h \in P_h$ and all $v_h \in V_h$, the following holds:*

$$(C_h v, q_h)_L \lesssim c(\beta, h)^{\frac{1}{2}} h^{-\frac{1}{2}} \|v\|_L |q_h|_{S^p}, \tag{2.12a}$$

$$(B_h^{\mathrm{T}} q, v_h)_L \lesssim \check{c}(\beta, h)^{\frac{1}{2}} (h^{-\frac{1}{2}} \|q\|_L + \|q\|_{L, \partial\Omega})(|v_h|_{S^u} + \|v_h\|_{\mu, \beta}), \tag{2.12b}$$

$$(A_h v, v_h)_L \lesssim c(\beta, h)^{\frac{1}{2}} h^{-\frac{1}{2}} \|v\|_L |v_h|_{S^u} + L_\beta \|v\|_L \|v_h\|_L + \|v\|_{\mu, \beta} \|v_h\|_{\mu, \beta}. \tag{2.12c}$$

Proof.
We only sketch the proof and refer to [7] for further insight. The bound (2.12a) results from

$$(C_h v, q_h)_L = (v, \nabla q_h)_L = \inf_{y_h \in V_h} (v, \nabla q_h - y_h)_L \leq \|v\|_L \inf_{y_h \in V_h} \|\nabla q_h - y_h\|_L.$$

Taking for y_h a quasi-interpolate of ∇q_h in V_h based on averaging and proceeding as in [7], we infer that $\inf_{y_h \in V_h} \|\nabla q_h - y_h\|_L \lesssim c(\beta, h)^{\frac{1}{2}} h^{-\frac{1}{2}} |q_h|_{S^p}$. To prove (2.12b), we first observe that

$$(B_h^{\mathrm{T}} q, v_h)_L = (q, \nabla \cdot v_h)_L + (q, \nu \cdot v_h)_{L, \partial\Omega}.$$

The first term in the right-hand side, say $\mathfrak{T}_1$, can be bounded using either the stabilization or the viscous term as

$$|\mathfrak{T}_1| \lesssim h^{-\frac{1}{2}} \|q\|_L \left(\max_{F \in \mathcal{F}_h^{\mathrm{int}}} \min(\xi_F^{-1}\beta_F^{-1}, h_F \mu^{-1}) \right)^{\frac{1}{2}} (|v_h|_{S^u} + \|v_h\|_{\mu, \beta}).$$

Then, observing that $\min(\xi_F^{-1}\beta_F^{-1}, h_F\mu^{-1}) = \min(\beta_F^{-1}, h_F\mu^{-1}) = \xi_F\beta_F^{-1}$ and proceeding similarly for the boundary term, we obtain (2.12b). Finally, for (2.12c), denoting by $\bar{\beta}$ the element-wise average of the velocity field β, we infer that

$$(A_h v, w_h)_L \lesssim \inf_{y_h \in V_h} \left\{ -(v, \bar{\beta} \cdot \nabla w_h - y_h)_L \right\} + (v, (\bar{\beta} - \beta) \cdot \nabla w_h)_L + \|v\|_{\mu, \beta} \|w_h\|_{\mu, \beta},$$

using Cauchy–Schwarz inequalities on the diffusive part and the boundary terms. For the convective terms, we conclude as above for the first term in the right-hand side (note that $\beta_{\nu, F} \leq \beta_F$), the Lipschitz property of β, and inverse inequalities. $\qquad\square$

For the proof of the following approximation results, we refer to [7]. For simplicity, we assume that the functions to approximate are smooth enough. We also use π_h to denote the L-orthogonal projection onto M_h as well as that onto V_h.

Lemma 2.2 (Approximation). *Let $k \geq 1$ be the polynomial degree. Assume that $v \in [H^{k+1}(\Omega)]^d$ and $q \in H^{k+1}(\Omega)$. Set $\beta_\Omega := \|\beta\|_{[L^\infty(\Omega)]^d}$. Then, the following holds:*

$$\|v - \pi_h v\|_L \lesssim h^{k+1} |v|_{[H^{k+1}(\Omega)]^d}, \tag{2.13a}$$

$$\|q - \pi_h q\|_L + h^{\frac{1}{2}} \|q - \pi_h q\|_{L, \partial\Omega} \lesssim h^{k+1} |q|_{H^{k+1}(\Omega)}, \tag{2.13b}$$

$$\|v - \pi_h v\|_{\mu, \beta} \lesssim c(\beta, h)^{\frac{1}{2}} h^{k+\frac{1}{2}} |v|_{[H^{k+1}(\Omega)]^d}, \tag{2.13c}$$

$$|v - \pi_h v|_{S^u} \lesssim \check{c}(\beta, h)^{\frac{1}{2}} \beta_\Omega h^{k+\frac{1}{2}} |v|_{[H^{k+1}(\Omega)]^d}, \tag{2.13d}$$

$$|q - \pi_h q|_{S^p} \lesssim \check{c}(\beta, h)^{\frac{1}{2}} h^{k+\frac{1}{2}} |q|_{H^{k+1}(\Omega)}. \tag{2.13e}$$

3. Monolithic time discretization

Let τ be the time step, taken to be constant for simplicity and such that $N\tau = t_{\mathrm{F}}$. We define the Courant number as

$$\mathrm{Co} := \frac{\beta_\Omega \tau}{h}. \tag{3.1}$$

In what follows, for $0 \leq n \leq N$, a superscript n indicates the values of a function at the discrete time $n\tau$, *e.g.*, $u^n = u(t^n)$ and $p^n = p(t^n)$. We assume at least that $u^n \in [H^2(\Omega)]^d$ and $p^n \in H^2(\Omega)$ for all $n \geq 1$.

In this section, we consider a BDF1 ($l = 1$) or BDF2 ($l = 2$) monolithic time discretization of the space semi-discrete problem (2.8a)–(2.8b). The fully discrete scheme takes the following form: For all $n \geq l - 1$, find $u_h^{n+1} \in V_h$ and $p_h^{n+1} \in P_h$ such that

$$\partial_\tau^l u_h^{n+1} + A_h u_h^{n+1} + S_h^u u_h^{n+1} + B_h^{\mathrm{T}} p_h^{n+1} = f_h^{n+1} \quad (\text{in } V_h), \tag{3.2a}$$

$$-B_h u_h^{n+1} + S_h^p p_h^{n+1} = 0 \qquad (\text{in } P_h), \tag{3.2b}$$

where $f_h := \pi_h f$, $\partial_\tau^1 u_h^{n+1} = \frac{1}{\tau}(u_h^{n+1} - u_h^n)$, and $\partial_\tau^2 u_h^{n+1} = \frac{1}{2\tau}(u_h^{n+1} - 4u_h^n + 3u_h^{n-1})$.

We now derive error estimates for the velocity and the pressure. Define the velocity error $e^n := u^n - u_h^n$ and the pressure error $\eta^n := p^n - p_h^n$. It is readily seen that the equations governing the velocity and pressure errors read as follows:

$$\pi_h \partial_\tau^l e^{n+1} + A_h e^{n+1} + S_h^u e^{n+1} + B_h^{\mathrm{T}} \eta^{n+1} = \pi_h \Psi_l^{n+1} \quad (\text{in } V_h), \tag{3.3a}$$

$$-B_h e^{n+1} + S_h^p \eta^{n+1} = 0 \qquad (\text{in } P_h), \tag{3.3b}$$

where $\Psi_l^n := \partial_\tau^l u^n - (\partial_t u)^n$ for all $n \geq 1$.

In what follows, we consider the discrete L^2-in-time (at the time nodes) norm of a space-time function z that we denote $\|z\|_{\ell^2(0,t_{\mathrm{F}};Z)}^2 := \tau \sum_{n=1}^N \|z(t^n)\|_Z^2$ where Z is some space of functions in space. We define the time-averaged pressure error $\bar{\eta}^N := N^{-1} \sum_{n=l}^N \eta^n$. To avoid technicalities with the initialization of the scheme, we neglect the error for $n \leq l - 1$. The discrete initial data u_h^0 can be chosen to be any L-stable approximation, and the approximation u_h^1 necessary to initialize BDF2 can be computed using one step of BDF1. Observe that it is not necessary to use the discretely divergence-free Stokes projection to initialize the scheme as suggested in [5], since we only use the energy stability and we only estimate the time-averaged $L^2(\Omega)$-error on the pressure, which is a weaker measure than the $L^2(0, t_{\mathrm{F}}; L^2(\Omega))$-norm considered in [5].

To simplify the pressure estimate, we assume that $\max(\mu, \beta_F h_F) \leq 1$ for all $F \in \mathcal{F}_h$, so that $c(\beta, h)h \leq 1$, that $\beta_\Omega \leq 1$, and that $t_{\mathrm{F}} \geq 1$.

Theorem 3.1 (Error estimates). *Assume that $u(t^n) \in [H^{k+1}(\Omega)]^d$ and $p(t^n) \in H^{k+1}(\Omega)$ for all $n \geq l$, and $\partial_t^{l+1} u \in L^2(Q)$, recalling that Q is the space-time cylinder $\Omega \times (0, t_{\mathrm{F}})$. Then, the following estimates hold:*

$$\|e^N\|_L + \left(\sum_{n \geq l} \tau \left(\|e^n\|_{\mu,\beta}^2 + |e^n|_{S^u}^2 + |\eta^n|_{S^p}^2 \right) \right)^{\frac{1}{2}}$$

$$\lesssim \left(c(\beta, h)^{\frac{1}{2}} + \check{c}(\beta, h)^{\frac{1}{2}} \beta_\Omega + t_{\mathrm{F}}^{\frac{1}{2}} L_\beta h^{\frac{1}{2}} \right) h^{k+\frac{1}{2}} \|u\|_{\ell^2(0,t_{\mathrm{F}};H^{k+1}(\Omega))}$$

$$+ \check{c}(\beta, h)^{\frac{1}{2}} h^{k+\frac{1}{2}} \|p\|_{\ell^2(0,t_{\mathrm{F}};H^{k+1}(\Omega))} + t_{\mathrm{F}}^{\frac{1}{2}} \tau^l \|\partial_t^{l+1} u\|_{L,Q}, \tag{3.4a}$$

$$\|\bar{\eta}^N\|_L \lesssim h^{k+1} \|\bar{p}^N\|_{H^{k+1}(\Omega)}$$

$$+ t_{\mathrm{F}}^{-\frac{1}{2}} \left(c(\beta, h)^{\frac{1}{2}} + \check{c}(\beta, h)^{\frac{1}{2}} \beta_\Omega + t_{\mathrm{F}}^{\frac{1}{2}} L_\beta h^{\frac{1}{2}} \right) h^{k+\frac{1}{2}} \|u\|_{\ell^2(0,t_{\mathrm{F}};H^{k+1}(\Omega))}$$

$$+ t_{\mathrm{F}}^{-\frac{1}{2}} \check{c}(\beta, h)^{\frac{1}{2}} h^{k+\frac{1}{2}} \|p\|_{\ell^2(0,t_{\mathrm{F}};H^{k+1}(\Omega))} + t_{\mathrm{F}}^{-\frac{1}{2}} \tau^l \|\partial_t^{l+1} u\|_{L,Q}. \tag{3.4b}$$

Proof.

The estimate (3.4a) can be derived using the arguments of [4], the boundedness estimates from Lemma 2.1, the approximation results from Lemma 2.2, and the standard truncation error estimates for the discrete time derivative. We detail here only the proof of (3.4b). Let $\bar{v}_p \in [H_0^1(\Omega)]^d$ be such that

$$\nabla\cdot\bar{v}_p = \bar{\eta}^N, \qquad \|\bar{v}_p\|_{[H^1(\Omega)]^d} \lesssim \|\bar{\eta}^N\|_L.$$

Then, using $y_h^n = \pi_h p^n - p_h^n$, and letting $\bar{y}_h^N$ and $\bar{p}^N$ be the discrete time averages of the functions y_h^n and p^n, we infer that

$$\begin{aligned}
\|\bar{\eta}^N\|_L^2 &= (\bar{\eta}^N, \nabla\cdot\bar{v}_p)_L = (\bar{\eta}^N, \nabla\cdot(\bar{v}_p - \pi_h\bar{v}_p))_L + (\bar{\eta}^N, \nabla\cdot\pi_h\bar{v}_p)_L \\
&= (\bar{p}^N - \pi_h\bar{p}^N, \nabla\cdot(\bar{v}_p - \pi_h\bar{v}_p))_L + (\bar{y}_h^N, \nabla\cdot(\bar{v}_p - \pi_h\bar{v}_p))_L + (\bar{\eta}^N, \nabla\cdot\pi_h\bar{v}_p)_L \\
&= -(\nabla(\bar{p}^N - \pi_h\bar{p}^N), \bar{v}_p - \pi_h\bar{v}_p)_L - (\bar{y}_h^N, C_h(\bar{v}_p - \pi_h\bar{v}_p))_L + (\bar{\eta}^N, \nabla\cdot\pi_h\bar{v}_p)_L.
\end{aligned}$$

Let us denote $\mathfrak{T}_{1,2,3}$ the three terms in the right-hand side. We first observe that

$$|\mathfrak{T}_1| \lesssim h^{k+1}|\bar{p}^N|_{H^{k+1}(\Omega)}\|\bar{\eta}^N\|_L.$$

The second term is bounded using (2.12a) leading to

$$|\mathfrak{T}_2| \lesssim c(\beta,h)^{\frac{1}{2}}h^{-\frac{1}{2}}\|\bar{v}_p - \pi_h\bar{v}_p\|_L|\bar{y}_h^N|_{S^p} \lesssim |\bar{y}_h^N|_{S_p}\|\bar{\eta}^N\|_L,$$

where we have used that $c(\beta,h)h \leq 1$ to simplify the estimate. Moreover, using the triangle inequality and a discrete Cauchy–Schwarz inequality in time leads to

$$|\bar{y}_h^N|_{S_p} \leq t_{\mathrm{F}}^{-\frac{1}{2}}\left(\sum_{n\geq l}\tau|y_h^n|_{S_p}^2\right)^{\frac{1}{2}}.$$

For the third term, we use $\mathfrak{T}_3 = -(B_h^{\mathrm{T}}\bar{\eta}^N, \pi_h\bar{v}_p)_L$ and we sum (3.3a) over n to infer that

$$\mathfrak{T}_3 = \frac{1}{N}\sum_{n\geq l}(\partial_\tau^l e^n + A_h e^n + S_h^u e^n + \Psi_l^n, \pi_h\bar{v}_p)_L.$$

Since $\pi_h\bar{v}_p$ does not depend on time, owing to the classical telescoping properties of BDF methods, we infer that $\frac{1}{N}\sum_{n\geq l}(\partial_\tau^l e^n, \pi_h\bar{v}_p)_L \lesssim t_{\mathrm{F}}^{-1}(\|e^N\|_L + \|e^{N-1}\|_L)\|\bar{\eta}^N\|_L$ (the second term is needed only for $l = 2$); note also that $t_{\mathrm{F}}^{-1} \leq t_{\mathrm{F}}^{-\frac{1}{2}}$ owing to the simplifying assumption $t_{\mathrm{F}} \geq 1$. We observe that (using again that $\beta_F h_F \leq 1$)

$$\begin{aligned}
(A_h e^n, \pi_h\bar{v}_p)_L &\lesssim (\|e^n\|_{\mu,\beta} + \|e^n\|_L)\|\bar{\eta}^N\|_L, \\
(S_h^u e^n, \pi_h\bar{v}_p)_L &\leq |e^n|_{S^u}|\pi_h\bar{v}_p|_{S^u} \lesssim |e^n|_{S^u}\max_{F\in\mathcal{F}_h}(\beta_F^{\frac{1}{2}}h_F^{\frac{1}{2}})\|\bar{v}_p\|_{[H^1(\Omega)]^d} \lesssim |e^n|_{S^u}\|\bar{\eta}^N\|_L.
\end{aligned}$$

Using a discrete Cauchy–Schwarz inequality in time, we infer that

$$\frac{1}{N}\sum_{n\geq l}(A_h e^n + S_h^u e^n, \pi_h\bar{v}_p)_L \lesssim t_{\mathrm{F}}^{-\frac{1}{2}}\left(\sum_{n\geq l}\tau(\|e^n\|_{\mu,\beta}^2 + \|e^n\|_L^2 + |e^n|_{S^u}^2)\right)^{\frac{1}{2}}\|\bar{\eta}^N\|_L.$$

Moreover, using the classical properties of the time truncation error in BDF methods, we infer that $(\Psi_l^n, \pi_h\bar{v}_p)_L \lesssim \tau^l\|\partial_t^{l+1}u\|_{L,Q^n}\|\bar{\eta}^N\|_L$, with $Q^n := \Omega \times [t^n, t^{n+1}]$. The pressure estimate now follows from the velocity estimate. $\square$

Remark 3.2 (High Reynolds number)**.** Observe that in the high Reynolds number regime and for smooth u and p, we recover the classical velocity estimate of order $h^{k+\frac{1}{2}} + \tau^l$, while the estimate on the time-average pressure is of the same order.

4. FRACTIONAL-STEP TIME DISCRETIZATION USING PRESSURE PROJECTION

Given $u_h^0 \in V_h$, $\widetilde{u}_h^0 \in \widetilde{V}_h$, and $p_h^0 \in P_h$, the BDF1 projection method consists in solving for all $n \geq 0$,

(1) an advection-diffusion problem yielding $u_h^{n+1} \in V_h$,

$$\frac{1}{\tau}(u_h^{n+1} - \pi_h\widetilde{u}_h^n) + A_h u_h^{n+1} + S_h^u(u_h^*) = f_h^{n+1} - B_h^{\mathrm{T}}p_h^n \quad (\text{in } V_h), \tag{4.1}$$

with the choice $u_h^* = u_h^{n+1}$ for implicit velocity stabilization or $u_h^* = \pi_h\widetilde{u}_h^n$ or $u_h^* = u_h^n$ for explicit velocity stabilization.

(2) A Poisson problem with homogeneous Neumann boundary conditions yielding $p_h^{n+1} \in P_h$ and $\widetilde{u}_h^{n+1} \in \widetilde{V}_h$,

$$\frac{1}{\tau}(\widetilde{u}_h^{n+1} - u_h^{n+1}) + C_h^{\mathrm{T}}(p_h^{n+1} - p_h^n) + \frac{1}{\tau}\widetilde{S}_h^p p_h^* = 0 \quad (\text{in } \widetilde{V}_h), \tag{4.2a}$$

$$C_h\widetilde{u}_h^{n+1} = 0 \quad (\text{in } M_h), \tag{4.2b}$$

with $p_h^* = p_h^{n+1}$ (implicit pressure stabilization) or $p_h^* = p_h^n$ (explicit pressure stabilization) and where $\widetilde{S}_h^p : M_h \to \widetilde{V}_h$ is such that for all $(q_h, \widetilde{v}_h) \in P_h \times \widetilde{V}_h$,

$$(\widetilde{S}_h^p q_h, \widetilde{v}_h)_L := \sum_{F \in \mathcal{F}_h^{\mathrm{int}}} \gamma_4 \xi_F \|\beta\|_{L^\infty(F)^d}^{-1} h_F^2 (\llbracket\nabla q_h\rrbracket, \llbracket\widetilde{v}_h\rrbracket)_{L,F}. \tag{4.3}$$

Since C_h^{T} is the restriction of the gradient operator to P_h, we obtain for all $(q_h, r_h) \in P_h \times P_h$, $(\widetilde{S}_h^p q_h, C_h^{\mathrm{T}}r_h)_L = (S_h^p q_h, r_h)_L$, so that

$$C_h\widetilde{S}_h^p = S_h^p. \tag{4.4}$$

Moreover, since V_h is H^1-conforming, for all $q_h \in M_h$, $\widetilde{S}_h^p q_h$ is L-orthogonal to V_h, that is, for all $(q_h, v_h) \in P_h \times V_h$, $(\widetilde{S}_h^p q_h, v_h)_L = 0$, so that

$$\pi_h\widetilde{S}_h^p = 0. \tag{4.5}$$

Finally, using a discrete trace inequality, we infer that there are C_2, C_3 such that for all $q_h \in P_h$,

$$\|\widetilde{S}_h^p q_h\|_L \leq C_2 \gamma_4^{\frac{1}{2}} \check{c}(\beta, h)^{\frac{1}{2}} h^{\frac{1}{2}} |q_h|_{S^p}. \tag{4.6}$$

Applying the projector π_h to (4.2a) at step n, using $\pi_h C_h^{\mathrm{T}} = B_h^{\mathrm{T}}$ and (4.5), and combining with (4.1) yields for $n \geq 1$,

$$\frac{1}{\tau}(u_h^{n+1} - u_h^n) + A_h u_h^{n+1} + S_h^u(u_h^*) = f_h^{n+1} - B_h^{\mathrm{T}}(2p_h^n - p_h^{n-1}) \quad (\text{in } V_h). \tag{4.7}$$

Moreover, applying the operator C_h to (4.2a) and using (4.2b) and (4.4) yields

$$C_h C_h^{\mathrm{T}}(p_h^{n+1} - p_h^n) = \frac{1}{\tau}\left(B_h u_h^{n+1} - S_h^p p_h^*\right) \quad (\text{in } P_h), \tag{4.8}$$

since $u_h^{n+1} \in V_h$ and C_h is an extension of B_h. Using equation (4.8) and (4.2a) we can derive an explicit expression for $\widetilde{u}_h^{n+1}$. For $p^* = p^n$, we get

$$\widetilde{u}_h^{n+1} = u_h^{n+1} - C_h^{\mathrm{T}}(C_h C_h^{\mathrm{T}})^{-1}(B_h u_h^{n+1} - S_h^p p_h^n) - \widetilde{S}_h^p p_h^n,$$

and for $p^* = p^{n+1}$,

$$\widetilde{u}_h^{n+1} = u_h^{n+1} - \tau(C_h^{\mathrm{T}} + \widetilde{S}_h^p)(\tau C_h C_h^{\mathrm{T}} + S_h^p)^{-1}(B_h u_h^{n+1} - S_h^p p_h^n) - \widetilde{S}_h^p p_h^n.$$

4.1. Stability

In this section we prove a discrete stability result for the projection scheme (4.2). We first prove a generic result without specifying u^* and p^* and then we detail the different explicit or implicit treatments of the stabilization terms.

Lemma 4.1 (Stability). *The following holds:*

$$
\begin{aligned}
&\frac{1}{2}\|\pi_h\widetilde{u}_h^{n+1}\|_L^2 - \frac{1}{2}\|\pi_h\widetilde{u}_h^n\|_L^2 + \frac{1}{2}\|u_h^{n+1} - \pi_h\widetilde{u}_h^n\|_L^2 + \tau(A_h u_h^{n+1}, u_h^{n+1})_L + \tau|u_h^{n+1}|_{S^u}^2 \\
&+ \frac{1}{2}\tau^2\|\nabla p_h^{n+1}\|_L^2 - \frac{1}{2}\tau^2\|\nabla p_h^n\|_L^2 + \frac{1}{2}\tau^2\|(I - \pi_h)\nabla(p_h^{n+1} - p_h^n)\|_L^2 + \tau|p_h^{n+1}|_{S^p}^2 \\
&= \tau(f_h^{n+1}, u_h^{n+1})_L + \tau(S_h^u(u_h^{n+1} - u_h^*), u_h^{n+1})_L + \tau(S_h^p(p_h^{n+1} - p_h^*), p_h^{n+1})_L.
\end{aligned} \tag{4.9}
$$

Proof.
Step 1. Testing (4.1) with τu_h^{n+1} yields

$$
\begin{aligned}
\frac{1}{2}\|u_h^{n+1}\|_L^2 - \frac{1}{2}\|\pi_h\widetilde{u}_h^n\|_L^2 + \frac{1}{2}\|u_h^{n+1} - \pi_h\widetilde{u}_h^n\|_L^2 + \tau(A_h u_h^{n+1}, u_h^{n+1})_L + \tau|u_h^{n+1}|_{S^u}^2 = \\
\tau(f_h^{n+1}, u_h^{n+1})_L + \tau(S_h^u(u_h^{n+1} - u_h^*), u_h^{n+1})_L - \tau(B_h^{\mathrm{T}} p_h^n, u_h^{n+1})_L.
\end{aligned} \tag{4.10}
$$

Step 2. Applying π_h to (4.2a) yields

$$
\pi_h\widetilde{u}_h^{n+1} - u_h^{n+1} + \tau B_h^{\mathrm{T}}(p_h^{n+1} - p_h^n) = 0. \tag{4.11}
$$

Applying B_h to this equation, we infer that

$$
B_h\pi_h\widetilde{u}_h^{n+1} - B_h u_h^{n+1} + \tau B_h B_h^{\mathrm{T}}(p_h^{n+1} - p_h^n) = 0. \tag{4.12}
$$

Applying C_h to (4.2a) and using (4.2b) yields

$$
B_h u_h^{n+1} = \tau C_h C_h^{\mathrm{T}}(p_h^{n+1} - p_h^n) + S_h^p p_h^*, \tag{4.13}
$$

and adding (4.13) to (4.12) leads to

$$
B_h\pi_h\widetilde{u}_h^{n+1} = \tau(C_h C_h^{\mathrm{T}} - B_h B_h^{\mathrm{T}})(p_h^{n+1} - p_h^n) + S_h^p p_h^*. \tag{4.14}
$$

Testing (4.13) with τp_h^n and recalling that C_h^{T} is the restriction of the gradient operator to P_h, we infer that

$$
\tau(B_h^{\mathrm{T}} p_h^n, u_h^{n+1})_L = \frac{1}{2}\tau^2\|\nabla p_h^{n+1}\|_L^2 - \frac{1}{2}\tau^2\|\nabla p_h^n\|_L^2 - \frac{1}{2}\tau^2\|\nabla(p_h^{n+1} - p_h^n)\|_L^2 + \tau(S_h^p p_h^*, p_h^n)_L. \tag{4.15}
$$

Step 3. Testing (4.11) with $\pi_h\widetilde{u}_h^{n+1}$ and using (4.14), we infer that

$$
\frac{1}{2}\|\pi_h\widetilde{u}_h^{n+1}\|_L^2 - \frac{1}{2}\|u_h^{n+1}\|_L^2 + \frac{1}{2}\tau^2\|\pi_h\nabla(p_h^{n+1} - p_h^n)\|_L^2 = -\tau^2\|(I - \pi_h)\nabla(p_h^{n+1} - p_h^n)\|_L^2 - \tau(S_h^p p_h^*, p_h^{n+1} - p_h^n)_L, \tag{4.16}
$$

since $\|\pi_h\widetilde{u}_h^{n+1} - u_h^{n+1}\|_L^2 = \tau^2\|\pi_h\nabla(p_h^{n+1} - p_h^n)\|_L^2$.
Step 4. Combining (4.10) with (4.15)–(4.16) and re-arranging terms yields (4.9). $\qquad\square$

4.2. Implicit or explicit of stabilization

We now apply Lemma 4.1 to the various choices for the arguments of the stabilization operators to show that different options are possible leading to slightly different CFL conditions. To formulate these CFL conditions, we observe using discrete trace and inverse inequalities, that for all $v_h \in V_h$,

$$|v_h|_{S^u} \leq C_4 \gamma_1^{\frac{1}{2}} \check{c}(\beta, h)^{\frac{1}{2}} \beta_\Omega^{\frac{1}{2}} h^{-\frac{1}{2}} \|v_h\|_L. \tag{4.17}$$

Corollary 4.2. *Take in Lemma 4.1 $u^* = u_h^{n+1}$ or $u^* = \pi_h \widetilde{u}_h^n$, or $u^* = u_h^n$ for the special case of piecewise linears (i.e., $k=1$). For the pressure stabilization, take $p^* = p_h^{n+1}$ or $p^* = p_h^n$. Then, the following holds:*

$$\|\pi_h \widetilde{u}_h^N\|_L^2 + \tau \sum_{n=0}^{N-1} \left(\|u_h^{n+1}\|_{\mu,\beta}^2 + |u_h^{n+1}|_{S^u}^2 \right) + \tau^2 \|\nabla p_h^N\|_L^2 + \tau \sum_{n=0}^{N-1} |p_h^{n+1}|_{S^p}^2$$

$$\lesssim \sum_{n=0}^{N-1} t_F \tau \|f_h^{n+1}\|_L^2 + \|\pi_h \widetilde{u}_h^0\|_L^2 + \tau^2 \|\nabla p_h^0\|_L^2, \tag{4.18}$$

provided the following standard hyperbolic CFL condition holds for the explicit treatment of the velocity:

$$\mathrm{Co} < \tfrac{1}{4}(C_4^2 \gamma_1 \check{c}(\beta, h))^{-1}, \tag{4.19}$$

and provided the following additional condition holds for the explicit treatment of the pressure:

$$C_2^2 \gamma_4 \check{c}(\beta, h) h \leq \tau, \tag{4.20}$$

with C_2 defined by (4.6).

Proof.
In the implicit case where $u^* = u_h^{n+1}$ and $p^* = p_h^{n+1}$, there is only one term in the right-hand side of (4.9) since the stabilization terms vanish. We obtain that

$$\sum_{n=0}^{N-1} \tau(f_h^{n+1}, u_h^{n+1})_L = \sum_{n=0}^{N-1} \tau(f_h^{n+1}, \widetilde{u}_h^{n+1})_L + \tau^2 \sum_{n=0}^{N-1}(f_h^{n+1}, \nabla(p_h^{n+1} - p_h^n))_L$$

$$\leq \frac{5}{2} t_F \sum_{n=0}^{N-1} \tau \|f_h^{n+1}\|_L^2 + \frac{1}{2} t_F^{-1} \sum_{n=0}^{N-1} \tau \|\pi_h \widetilde{u}_h^{n+1}\|_L^2 + \frac{1}{2} t_F^{-1} \sum_{n=0}^{N-1} \tau^3 \|\nabla p_h^{n+1}\|_L^2 + \frac{1}{4} t_F^{-1} \tau^3 \|\nabla p_h^0\|_L^2,$$

and (4.18) is an immediate consequence of the discrete Gronwall's lemma, observing that $\tau/t_F \leq 1$ so that the term $\frac{1}{2}(\tau/t_F)(\|\pi_h \widetilde{u}_h^N\|^2 + \tau^2 \|\nabla p_h^N\|_L^2)$ in the righ-hand side can be absorbed in the left-hand side. Taking $u_h^* = \pi_h \widetilde{u}_h^n$, the second term on the right-hand side of (4.9) is absorbed by the third term in the left-hand side owing to (4.19) since

$$\tau(S_h^u(u_h^{n+1} - \pi_h \widetilde{u}_h^n), u_h^{n+1})_L \leq C_4^2 \gamma_1 \check{c}(\beta, h) \mathrm{Co} \|u_h^{n+1} - \pi_h \widetilde{u}_h^n\|_L^2 + \frac{1}{4} \tau |u_h^{n+1}|_{S^u}^2.$$

Taking $u_h^* = u_h^n$ is feasible for piecewise linears. To see this recall that by equation (4.11), $u_h^n = \pi_h \widetilde{u}_h^n - \tau \pi_h \nabla(p_h^{n+1} - p_h^n)$. For $k=1$, the following holds:

$$(S_h^u(u_h^{n+1} - u_h^n), u_h^{n+1})_L = (S_h^u(u_h^{n+1} - \pi_h \widetilde{u}_h^n), u_h^{n+1})_L + (S_h^u \tau(I - \pi_h)\nabla(p_h^{n+1} - p_h^n), u_h^{n+1})_L,$$

since $S_h^u(\nabla(p_h^{n+1} - p_h^n))$ vanishes because $\nabla(p_h^{n+1} - p_h^n)$ is piece-wise constant. The first contribution on the right-hand side is absorbed by the third term in the left-hand side of (4.9) using (4.19) as before. For the second term, we deduce from (4.17) that

$$\tau(S_h^u \tau(I - \pi_h)\nabla(p_h^{n+1} - p_h^n), u_h^{n+1})_L \leq \tau \frac{1}{4}|u_h^{n+1}|_{S^u}^2 + C_4^2 \gamma_1 \check{c}(\beta, h) \mathrm{Co}\|\tau(I - \pi_h)\nabla(p_h^{n+1} - p_h^n)\|_L^2.$$

The first term can be absorbed by the contribution from the velocity stabilization in the left-hand side, and the second one can be absorbed by the second to last term in the left-hand side of (4.9) still using (4.19). Finally, taking $p_h^* = p_h^n$, we observe that

$$\tau(S_h^p(p_h^{n+1} - p_h^n), p_h^{n+1})_L = \tau((I - \pi_h)\nabla(p_h^{n+1} - p_h^n), \widetilde{S}_h^p p_h^{n+1})_L$$

$$\leq \tau^2 \|(I - \pi_h)\nabla(p_h^{n+1} - p_h^n)\|_L^2 + C_2^2 \gamma_4 \check{c}(\beta, h) h |p_h^{n+1}|_{S^p}^2,$$

and the last term can be absorbed in the left-hand side using (4.20).   □

Remark 4.3 (Reverse CFL). For high-Reynolds flows, condition (4.20) yields a reverse hyperbolic CFL condition; it can be made compatible with other bounds on the Courant number by choosing γ_4 small enough. In the low-Reynolds regime, this condition becomes milder, of the form $h^2 \lesssim \mu\tau$.

Remark 4.4 (Stabilized Darcy). Since we use equal-order interpolation, the projection step, which is equivalent to a Darcy problem, has inf-sup constant that tends to zero as $h \to 0$ unless stabilization is applied. Corollary 4.2 shows that applying the stabilization operator with the pressure from the previous time step is enough to restore uniform inf-sup stability.

Remark 4.5 (Control on u_h^N). It also follows from (4.18) that control of $\pi_h \widetilde{u}_h^N$ is sufficient to control u_h^N, which justifies the analysis in the variable $\pi_h \widetilde{u}_h^N$. Indeed, let us first note that since (4.18) holds for all N, we infer that

$$\max_{n \in \{0,\dots,N\}} \|\pi_h \widetilde{u}_h^n\|_L^2 + \max_{n \in \{0,\dots,N\}} \tau^2 \|\nabla p_h^n\|_L^2 \lesssim \sum_{n=0}^{N-1} \tau \|f_h^{n+1}\|_L^2 + \frac{1}{2}\|\pi_h \widetilde{u}_h^0\|_L^2 + \frac{1}{2}\tau^2 \|\nabla p_h^0\|_L^2.$$

Owing to (4.11) we infer that

$$\|u_h^N\|_L^2 \lesssim \|\pi_h \widetilde{u}_h^N\|_L^2 + \tau^2 \|\nabla p_h^N\|_L^2 + \tau^2 \|\nabla p_h^{N-1}\|_L^2 \lesssim \max_{n \in \{0,\dots,N\}} \|\pi_h \widetilde{u}_h^n\|_L^2 + \max_{n \in \{0,\dots,N\}} \tau^2 \|\nabla p_h^n\|_L^2,$$

which leads to the desired stability bound on $\|u_h^N\|_L^2$ and later to the same error estimates for $\|u_h^N\|_L^2$ as for $\|\pi_h \widetilde{u}_h^N\|_L^2$. Hence, it suffices to consider the variable $\pi_h \widetilde{u}_h^N$, keeping in mind that all the estimates carry over without modification to u_h^N.

4.3. Error analysis

The error analysis follows in a relatively straightforward fashion, using the stability result (4.18), followed by consistency (Galerkin orthogonality) and the boundedness result from Lemma 2.1. The order in time is a consequence of the truncation error of the BDF1 scheme and the first-order splitting error of the incremental pressure-projection method. We first introduce a suitable error equation, with approximation errors and truncation errors as data. Then we apply the stability result from the previous section to this error equation, repeating some steps for enhanced clarity. The error estimates are then obtained using consistency followed by boundedness; convergence rates finally result from the approximation properties of finite elements.

To derive the error equation, we set

$$e_h^n := u_h^n - \pi_h u^n, \qquad e_\pi^n := u^n - \pi_h u^n, \tag{4.21}$$

$$\eta_h^n := p_h^n - \pi_h p^n, \qquad \eta_\pi^n := p^n - \pi_h p^n, \tag{4.22}$$

together with $\widetilde{e}_h^n := \widetilde{u}_h^n - \pi_h u^n$ and $\widetilde{e}_\pi^n := e_\pi^n$. We introduce the truncation errors

$$\Psi_1^n := \partial_t u^n - \frac{1}{\tau}(u^{n+1} - u^n), \qquad \Psi_2^n := p^{n+1} - p^n. \tag{4.23}$$

Finally, we set

$$\zeta_h^n := \eta_h^n - \pi_h \Psi_2^n, \tag{4.24}$$

so that $\zeta_h^n = p_h^n - \pi_h p^{n+1}$. Owing to Remark 4.5 we infer that

$$\|\widetilde{e}_h^n\|_L \lesssim \|e_h^n\|_L + \tau \|\nabla \eta_h^n\|_L + \tau \|\nabla \eta_h^{n-1}\|_L + \tau \|\nabla \pi_h \Psi_2^{n-1}\|_L. \tag{4.25}$$

We also recall the following standard truncation error estimates

$$\sum_{n=1}^N \tau(\|\Psi_1^n\|_L^2 + \|\nabla \Psi_2^n\|_L^2) \lesssim \tau^2(\|\partial_t^2 u\|_{\ell^2(0,t_\mathrm{F};L)}^2 + \|\partial_t \nabla p\|_{\ell^2(0,t_\mathrm{F};L)}^2). \tag{4.26}$$

Lemma 4.6 (Error equations). *The velocity error equation takes the form*

$$\frac{1}{\tau}(e_h^{n+1} - \pi_h \widetilde{e}_h^n) + A_h e_h^{n+1} + S_h^u(e_h^*) + B_h^\mathrm{T} \zeta_h^n = B_h^\mathrm{T} \eta_\pi^{n+1} + \pi_h \Psi_1^n + A_h e_\pi^{n+1} + S_h^u e_\pi^*, \tag{4.27}$$

with $e_h^* = e_h^{n+1}$ and $e_\pi^* = e_\pi^{n+1}$ for implicit velocity stabilization, while $e_h^* = \pi_h \widetilde{e}_h^n$ or $e_h^* = e_h^n$ and $e_\pi^* = e_\pi^n$ for explicit velocity stabilization. Moreover, the pressure error equation takes the form

$$\frac{1}{\tau}(\widetilde{e}_h^{n+1} - e_h^{n+1}) + C_h^\mathrm{T}(\eta_h^{n+1} - \zeta_h^n) + \frac{1}{\tau}\widetilde{S}_h^p \eta_h^* = \frac{1}{\tau}\widetilde{S}_h^p \eta_\pi^*, \tag{4.28a}$$

$$C_h \widetilde{e}_h^{n+1} = C_h e_\pi^{n+1}, \tag{4.28b}$$

where $\eta_h^* = \eta_h^{n+1}$ and $\eta_\pi^* = \eta_\pi^{n+1}$ for implicit pressure stabilization and $\eta_h^* = \eta_h^n$ and $\eta_\pi^* = \eta_\pi^n$ for explicit pressure stabilization.

Proof.
Use the fact that $\pi_h \partial_t u^{n+1} + A_h u^{n+1} + B_h^\mathrm{T} p^{n+1} = f_h^{n+1}$ to prove (4.27). Moreover, (4.28a) is directly verified by adding and subtracting $\pi_h u^{n+1}$ and $\pi_h p^{n+1}$. Finally, use the fact that $C_h u^{n+1} = 0$ to prove (4.28b). □

Theorem 4.7 (Error estimate). *Assume that $(u,p) \in [H^{k+1}(\Omega)]^{d+1}$ for the solution of (1.1). Let u_h^n and p_h^n be the solutions of (4.1)-(4.2b), $n = 1, \dots, N$, with mesh-parameters satisfying the assumptions of Corollary 4.2 if an explicit treatment of stabilization is employed. Then the following holds with $e^n := u_h^n - u(t^n)$, $\eta^n := p_h^n - p(t^n)$ and $\bar{\eta}^N := N^{-1} \sum_{n=1}^N \eta^n$:*

$$\|e^N\|_L + \tau \|\nabla \eta^N\|_L + \left(\sum_{n=1}^N \tau(\|e^n\|_{\mu,\beta}^2 + |e^n|_{S^u}^2 + |\eta|_{S^p}^2) \right)^{\frac{1}{2}}$$

$$\lesssim \left(c(\beta,h)^{\frac{1}{2}} + \check{c}(\beta,h)^{\frac{1}{2}} \beta_\Omega + t_\mathrm{F}^{\frac{1}{2}} L_\beta h^{\frac{1}{2}} \right) h^{k+\frac{1}{2}} \|u\|_{\ell^2(0,t_F;H^{k+1}(\Omega))}$$

$$+ \check{c}(\beta,h)^{\frac{1}{2}} h^{k+\frac{1}{2}} \|p\|_{\ell^2(0,t_F;H^{k+1}(\Omega))} + t_\mathrm{F}^{\frac{1}{2}} \tau(\|\partial_t^2 u\|_{L,Q} + \|\partial_t \nabla p\|_{L,Q}), \tag{4.29a}$$

$$\|\bar{\eta}^N\|_L \lesssim h^{k+1} \|\bar{p}^N\|_{H^{k+1}(\Omega)}$$

$$+ t_\mathrm{F}^{-\frac{1}{2}} \left(c(\beta,h)^{\frac{1}{2}} + \check{c}(\beta,h)^{\frac{1}{2}} \beta_\Omega + t_\mathrm{F}^{\frac{1}{2}} L_\beta h^{\frac{1}{2}} \right) h^{k+\frac{1}{2}} \|u\|_{\ell^2(0,t_F;H^{k+1}(\Omega))}$$

$$+ t_\mathrm{F}^{-\frac{1}{2}} \check{c}(\beta,h)^{\frac{1}{2}} h^{k+\frac{1}{2}} \|p\|_{\ell^2(0,t_F;H^{k+1}(\Omega))} + \tau(\|\partial_t^2 u\|_{L,Q} + \|\partial_t \nabla p\|_{L,Q}). \tag{4.29b}$$

Proof.

After a standard decomposition of the error in an approximation part e_π^n, η_π^n and a discrete part e_h^n, η_h^n and recalling equation (4.25), we observe that it is enough to bound for all N the discrete error

$$\|\pi_h \widetilde{e}_h^N\|_L^2 + \tau^2 \|\nabla \eta_h^N\|_L^2 + \tau \sum_{n=1}^N (\|e_h^{n+1}\|_{\mu,\beta}^2 + |e_h^{n+1}|_{S^u}^2 + \tau |\eta_h^{n+1}|_{S^p}^2). \tag{4.30}$$

Step 1. Multiplying (4.27) by τe_h^{n+1} yields

$$\frac{1}{2}\|e_h^{n+1}\|_L^2 - \frac{1}{2}\|\pi_h \widetilde{e}_h^n\|_L^2 + \frac{1}{2}\|e_h^{n+1} - \pi_h \widetilde{e}_h^n\|_L^2 + \tau(A_h e_h^{n+1}, e_h^{n+1})_L^2 + \tau |e_h^{n+1}|_{S^u}^2 =$$
$$- \tau(B_h^{\mathrm{T}} \zeta_h^n, e_h^{n+1})_L + \mathfrak{T}_1 + \ldots + \mathfrak{T}_5, \quad (4.31)$$

with

$$\begin{aligned}
\mathfrak{T}_1 &= \tau(B_h^{\mathrm{T}} \eta_\pi^{n+1}, e_h^{n+1})_L, \\
\mathfrak{T}_2 &= \tau(\Psi_1^n, e_h^{n+1})_L, \\
\mathfrak{T}_3 &= \tau(S_h^u(e_h^{n+1} - e_h^*), e_h^{n+1})_L, \\
\mathfrak{T}_4 &= \tau(A_h e_\pi^{n+1}, e_h^{n+1})_L, \\
\mathfrak{T}_5 &= \tau(S_h^u e_\pi^*, e_h^{n+1})_L.
\end{aligned}$$

$\mathfrak{T}_1$ is handled using equation (2.12b), exploiting the stabilization on the divergence and on the normal component at the boundary, followed by Young's inequality, absorbing the term $\tau |e_h^{n+1}|_{S^u}^2$ in the left-hand side. $\mathfrak{T}_2$ is handled by Gronwall's inequality; $\mathfrak{T}_3$ is handled as in Section 4.2, depending on the choice of velocity stabilization; $\mathfrak{T}_4$ is controlled using (2.12c), leading to the term $\tau(\|e_h^{n+1}\|_{\mu,\beta}^2 + |e_h^{n+1}|_{S^u}^2)$ that we absorb in the left-hand side and a term of the form $L_\beta \|e_h^{n+1}\|_L^2$ that is treated using Gronwall's inequality. Finally $\mathfrak{T}_5$ is controlled using a Cauchy–Schwarz inequality and Young's inequality and absorbing the term $\tau |e_h^{n+1}|_{S^u}^2$ in the left-hand side.

Step 2. Applying π_h to (4.28a) yields

$$(\pi_h \widetilde{e}_h^{n+1} - e_h^{n+1}) + \tau B_h^{\mathrm{T}}(\eta_h^{n+1} - \zeta_h^n) = 0. \tag{4.32}$$

Applying B_h to this equation leads to

$$B_h \pi_h \widetilde{e}_h^{n+1} - B_h e_h^{n+1} + \tau B_h B_h^{\mathrm{T}}(\eta_h^{n+1} - \zeta_h^n) = 0. \tag{4.33}$$

Applying C_h to (4.28a) and using (4.28b), we infer that

$$C_h e_\pi^{n+1} - B_h e_h^{n+1} + \tau C_h C_h^{\mathrm{T}}(\eta_h^{n+1} - \zeta_h^n) + S_h^p(\eta_h^* - \eta_\pi^*) = 0. \tag{4.34}$$

Subtracting (4.34) and (4.33),

$$B_h \pi_h \widetilde{e}_h^{n+1} = \tau(C_h C_h^{\mathrm{T}} - B_h B_h^{\mathrm{T}})(\eta_h^{n+1} - \zeta_h^n) + C_h e_\pi^{n+1} + S_h^p(\eta_h^* - \eta_\pi^*). \tag{4.35}$$

Testing (4.34) with ζ_h^n yields

$$\frac{1}{2}\tau^2 \|\nabla \eta_h^{n+1}\|_L^2 - \frac{1}{2}\tau^2 \|\nabla \zeta_h^n\|_L^2 - \frac{1}{2}\tau^2 \|\nabla(\eta_h^{n+1} - \zeta_h^n)\|_L^2 + \tau(S_h^p(\eta_h^* - \eta_\pi^*), \zeta_h^n)_L$$
$$= \tau(B_h^{\mathrm{T}} \zeta_h^n, e_h^{n+1})_L - \tau(C_h e_\pi^{n+1}, \zeta_h^n)_L.$$

Step 3. Testing (4.32) with $\pi_h \widetilde{e}_h^{n+1}$ yields

$$\frac{1}{2}\|\pi_h \widetilde{e}_h^{n+1}\|_L^2 - \frac{1}{2}\|e_h^{n+1}\|_L^2 + \frac{1}{2}\|\pi_h \widetilde{e}_h^{n+1} - e_h^{n+1}\|_L^2 = -\tau(B_h^{\mathrm{T}}(\eta_h^{n+1} - \zeta_h^n), \pi_h \widetilde{e}_h^{n+1})_L,$$

and using

$$\|\pi_h \widetilde{e}_h^{n+1} - e_h^{n+1}\|_L^2 = \tau^2 \|\pi_h \nabla(\eta_h^{n+1} - \zeta_h^n)\|_L^2 \tag{4.36}$$

together with (4.35) for the right-hand side, we arrive at

$$\frac{1}{2}\|\pi_h \widetilde{e}_h^{n+1}\|_L^2 - \frac{1}{2}\|e_h^{n+1}\|_L^2 + \frac{1}{2}\tau^2\|\pi_h \nabla(\eta_h^{n+1} - \zeta_h^n)\|_L^2 = -\tau^2\|(I - \pi_h)\nabla(\eta_h^{n+1} - \zeta_h^n)\|_L^2$$
$$- \tau(C_h e_\pi^{n+1}, \eta_h^{n+1} - \zeta_h^n)_L - \tau(S_h^p(\eta_h^* - \eta_\pi^*), \eta_h^{n+1} - \zeta_h^n)_L.$$

Step 4. Final combination. We infer that

$$\frac{1}{2}\|\pi_h \widetilde{e}_h^{n+1}\|_L^2 - \frac{1}{2}\|\pi_h \widetilde{e}_h^n\|_L^2 + \frac{1}{2}\|e_h^{n+1} - \pi_h \widetilde{e}_h^n\|_L^2 + \tau\|e_h^{n+1}\|_A^2 + \tau|e_h^{n+1}|_{S^u}^2$$
$$+ \frac{1}{2}\tau^2\|\nabla\eta_h^{n+1}\|_L^2 - \frac{1}{2}\tau^2\|\nabla\zeta_h^n\|_L^2 + \frac{1}{2}\tau^2\|(I - \pi_h)\nabla(\eta_h^{n+1} - \zeta_h^n)\|_L^2 + \tau|\eta_h^{n+1}|_{S^p}^2$$
$$= \mathfrak{T}_1 + \ldots + \mathfrak{T}_8,$$

with

$$\mathfrak{T}_6 = -\tau(C_h e_\pi^{n+1}, \eta_h^{n+1})_L,$$
$$\mathfrak{T}_7 = \tau(S_h^p \eta_h^{n+1}, \eta_\pi^*)_L,$$
$$\mathfrak{T}_8 = \tau(S_h^p \eta_h^{n+1}, \eta_h^{n+1} - \eta_\pi^*)_L.$$

The lack of a telescoping form for $\frac{1}{2}\tau^2\|\nabla\eta_h^{n+1}\|_L^2 - \frac{1}{2}\tau^2\|\nabla\zeta_h^n\|_L^2$ is not a problem since by a triangle inequality, we infer that

$$\|\nabla\zeta_h^n\|_L^2 \le (1 + \tau)\|\nabla\eta_h^n\|_L^2 + (1 + \tau^{-1})\|\nabla\pi_h\Psi_2^n\|_L^2, \tag{4.37}$$

the first term is handled by Gronwall's inequality and the second yields an $O(\tau)$-error. The term $\mathfrak{T}_6$ is bounded using (2.12a) and the term $\mathfrak{T}_7$ by the Cauchy–Schwarz inequality. The pressure stabilization contributions are then absorbed in the left-hand side. The term $\mathfrak{T}_8$ is treated as detailed in Section 4.2.

Collecting the above bounds, we obtain the inequality

$$\|\pi_h \widetilde{e}_h^{n+1}\|_L^2 - \|\pi_h \widetilde{e}_h^n\|_L^2 + \tau^2\|\nabla\eta_h^{n+1}\|_L^2 - \tau^2\|\nabla\eta_h^n\|_L^2 + \tau\|e_h^{n+1}\|_{\mu,\beta}^2 + \tau|e_h^{n+1}|_{S^u}^2 + \tau|\eta_h^{n+1}|_{S^p}^2$$
$$\lesssim \tau\check{c}(\beta, h)(h^{-1}\|\eta_\pi^{n+1}\|_L^2 + \|\eta_\pi^{n+1}\|_{L,\partial\Omega}^2)$$
$$+ \tau(c(\beta, h_F)h^{-1} + L_\beta^2 t_F)\|e_\pi^{n+1}\|_L^2 + \tau\|e_\pi^{n+1}\|_{\mu,\beta}^2$$
$$+ \tau(|e_\pi^*|_{S^u}^2 + |\eta_\pi^*|_{S^p}^2) + \tau t_F(\|\Psi_1^n\|_L^2 + \|\nabla\Psi_2^n\|_L^2)$$
$$+ \tau t_F^{-1}(\|e_h^{n+1}\|_L^2 + \tau^2\|\nabla\eta_h^{n+1}\|_L^2).$$

We add and subtract $\pi_h \widetilde{e}_h^{n+1}$ in $\|e_h^{n+1}\|_L^2$ in the last term in the right-hand side, and we use a triangle inequality, (4.36), and (4.37). We obtain the inequality

$$\tau t_F^{-1}(\|e_h^{n+1}\|_L^2 + \tau^2\|\nabla\eta_h^{n+1}\|_L^2)$$
$$\le 2\tau t_F^{-1}(\|\pi_h \widetilde{e}_h^{n+1}\|_L^2 + \|\pi_h \widetilde{e}_h^{n+1} - e_h^{n+1}\|_L^2 + \tau^2\|\nabla\eta_h^{n+1}\|_L^2)$$
$$\le 2\tau t_F^{-1}(\|\pi_h \widetilde{e}_h^{n+1}\|_L^2 + 5(1 + \tau)\tau^2\|\nabla\eta_h^{n+1}\|_L^2 + 2(1 + \tau^{-1})\tau^2\|\nabla\pi_h\Psi_2^n\|_L^2).$$

Now assume that τ is sufficiently small so that the $\|\pi_h \widetilde{e}_h^N\|_L^2 + \tau^2\|\nabla\eta_h^N\|_L^2$ contribution of the right hand side can be absorbed in the left hand side. Then the velocity error estimate follows after summing over n, applying Gronwall's Lemma and bounding the approximation errors using Lemma 2.2.

To prove the estimate on the time-averaged L^2-error on the pressure, we observe that the following error representation holds for all $1 \le n \le N - 1$:

$$\pi_h e^{n+1} - \pi_h e^n + \tau A_h e^{n+1} + \tau S_h^u(u_h^*) = \pi_h(u(t^{n+1}) - u(t^n) - \tau\partial_t u(t^{n+1})) - \tau B_h^{\mathrm{T}}\eta^{n+1}$$
$$+ \tau B_h^{\mathrm{T}}(\eta^{n+1} - 2\eta^n + \eta^{n-1}) + \tau B_h^{\mathrm{T}}(p(t^{n+1}) - 2p(t^n) + p(t^{n-1})). \tag{4.38}$$

Following the arguments of Theorem 3.1, we let $\bar{v}_p \in [H_0^1(\Omega)]^d$ be such that

$$\nabla \cdot \bar{v}_p = \bar{\eta}^N, \quad \|\bar{v}_p\|_{H^1(\Omega)} \lesssim \|\bar{\eta}^n\|_L.$$

Then using $y_h^n = \pi_h p^n - p_h^n$ we infer that

$$\|\bar{\eta}^N\|_L^2 = (\nabla(\bar{p}^n - \bar{\pi}_h p^n), \bar{v}_p - \pi_h \bar{v}_p)_L + (\bar{y}_h^n, C_h(\bar{v}_p - \pi_h \bar{v}_p))_L$$

$$+ t_F^{-1} \tau \sum_{n=1}^{N-1} \Big[(\partial_\tau^1 e^{n+1} + A_h e^{n+1} + S_h^u u_h^*, \pi_h \bar{v}_p)_L + (\partial_t u(t^n) - \tau^{-1}(u(t^n) - u(t^{n-1})), \pi_h \bar{v}_p)_L$$

$$- (B_h^{\mathrm{T}}(\eta^{n+1} - 2\eta^n + \eta^{n-1}), \pi_h \bar{v}_p)_L + (B_h^{\mathrm{T}}(p(t^{n+1}) - 2p(t^n) + p(t^{n-1})), \pi_h \bar{v}_p)_L \Big].$$

The only terms that differ from the monolithic case are those in the last line. We observe that telescoping the sum and using Poincaré's inequality leads to

$$\tau \sum_{n=1}^{N-1} (B_h^{\mathrm{T}}(\eta^{n+1} - 2\eta^n + \eta^{n-1}), \pi_h \bar{v}_p)_L = \tau(B_h^{\mathrm{T}}(\eta^N + \eta^{N-1} - \eta^1 + \eta^0), \pi_h \bar{v}_p)_L$$

$$\lesssim \tau(\|\nabla \eta^N\|_L + \|\nabla \eta^{N-1}\|_L) \|\pi_h \bar{v}_p\|_{H^1(\Omega)}$$
$$+ \tau(\pi_h p(t^1) - p(t^1) - \pi_h p(t^0) + p(t^0), \nabla \cdot \pi_h \bar{v}_p)_L$$
$$- \tau(\pi_h p(t^1) - p(t^1) - \pi_h p(t^0) + p(t^0), \nu \cdot (\pi_h \bar{v}_p - \bar{v}_p))_{L,\partial\Omega}$$
$$\lesssim \tau(\|\nabla \eta^N\|_L + \|\nabla \eta^{N-1}\|_L + h\|\nabla p(t^1)\|_L + h\|\nabla p_0\|_L) \|\bar{v}_p\|_{H^1(\Omega)},$$

where $\tau(\|\nabla \eta^N\|_L + \|\nabla \eta^{N-1}\|_L)$ is bounded in the first part of the proof. We use that $\|\nabla p(t^1)\|_L + \|\nabla p_0\|_L \lesssim \|\partial_t \nabla p\|_{L,Q}$ to conclude. $\square$

Remark 4.8. In the high Reynolds number regime, the satisfaction of the divergence-free condition relies on the stabilization term (2.7a). Expliciting only the dependence of the upper bound on h and τ in the error bound for $|e^n|_{S_u}$, we may write the asymptotics of $\nabla \cdot u_h^{n+1}$ as

$$\left(\sum_{n=1}^N \|h^{\frac{1}{2}} \nabla \cdot u_h^n\|_L^2 \right)^{\frac{1}{2}} \lesssim (h^{k+\frac{1}{2}} + \tau).$$

It follows that the choice $\tau \sim h^{k+\frac{1}{2}}$ gives a uniform h^k convergence rate on the divergence of u_h^n.

5. Numerical results

We illustrate the theoretical results on three test cases at different Reynolds numbers using piece-wise affine approximations ($k = 1$) for both velocity and pressure. In all cases we consider the Navier–Stokes equations in two space dimensions with unit density. The convective term is handled using extrapolation, taking the form $(u^* \cdot \nabla) u_h^{n+1}$ with $u^* = u_h^n$ or $u^* = 2u_h^n - u_h^{n-1}$. No fixed point iterations are performed. We have considered the following test cases:

- academic 2D solution at Re $= 10^5$;
- flow around a cylinder at Re $= 10^2$;
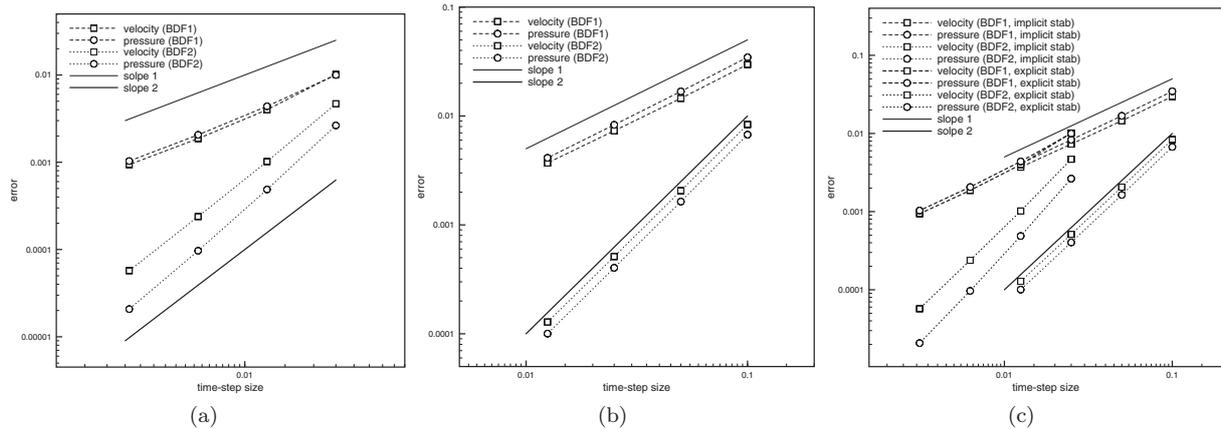- Kelvin–Helmholtz instability at Re $= 10^4$.

FIGURE 1. Convergence plot for the fractional-step method applied to the problem defined by the exact solution (5.1). (a) Explicit velocity stabilization; (b) implicit velocity stabilization. Dotted (resp., dashed) lines correspond to the fractional-step method using BDF2 (resp., BDF1). Solid lines mark first- and second-order slopes. Circle markers indicate L^2-norm errors on the velocity and square markers L^2-norm errors on the pressure. In (c) all the curves are collected in one graph for comparison. Here, the dash-dot curve indicates the BDF1 scheme, and dash-dot-dot curve indicates the BDF2 scheme, both with explicit treatment of the velocity stabilization.

The stabilization parameters involved in (2.6)-(2.7) have been set to $\gamma_1 = 20$, $\gamma_2 = \gamma_3 = \gamma_4 = 10^{-2}$ and $\widetilde{\gamma}_3 = 0$. Numerical tests not reported here indicate that taking $\widetilde{\gamma}_3 > 0$ has little influence on the results reported below. These tests also indicate that the tuning of the discretization parameters when the pressure stabilization is treated explicitly so that the method is both stable and accurate in all regimes are too delicate to be of practical use. Therefore, we do not report results with an explicit treatment of the pressure stabilization. Instead, an example showing the effect of explicit treatment of the velocity stabilization on the accuracy is presented. Although the theoretical results for the fractional-step method presented above are valid only for first-order BDF1 time scheme, we present numerical examples also for the BDF2 time scheme. Observe that the stability result from Lemma 4.1 remains valid in this case, but the order of the scheme is not improved due to the first-order splitting error.

5.1. Academic 2D solution at $\mathrm{Re} = 10^5$

This academic test case was used in [19] to show the effect of stabilization on the accuracy of a projection-based fractional-step solver for the Navier–Stokes equations. Let Ω be the unit square and set

$$\begin{cases} u_{\mathrm{ex}} = u(x,y)g(t), \quad p_{\mathrm{ex}} = -\frac{1}{4}\big(\cos(2x) + \cos(2y)\big)g^2(t), \\ u(x,y) = \big(-\cos(x)\sin(y), \quad \sin(x)\cos(y)\big)^{\mathrm{T}}, \quad g(t) = \sin(2t). \end{cases} \tag{5.1}$$

It is straightforward to verify that this is the exact solution of the Navier–Stokes equations driven by the body forces $f = u(x,y)(g'(t) + 2g(t)/\mathrm{Re})$. Dirichlet boundary conditions are imposed on the velocities on $\partial\Omega$ according to (5.1). We have performed computations using the fractional-step method and BDF1 time stepping or BDF2 time stepping combined with either explicit or implicit treatment of the velocity stabilization in each case. In the implicit case we have set $\tau = h \in \{0.1/2^i\}_{i=0}^3$, whereas in the explicit case we have set $\tau = \mathrm{Co}\beta_\Omega^{-1}h$ with Co fixed (approximately) to the largest time step for which the scheme was stable, namely, $(\tau, h) \in \{(2.5 \times 10^{-2}/2^i, 0.2/2^i)\}_{i=0}^3$. The results are reported in Figure 1. Observe that the points on the graphs

correspond to the same meshes in the two cases. The values on the x-axis correspond to time step sizes and those on the y-axis to the L^2-errors on the velocity (*circles*) and the pressure (*squares*). The curves corresponding to BDF1 time discretization are dashed and the curves corresponding to BDF2 time discretization are dotted. It follows from the graphics that in the case of BDF1, the reduced time step imposed by the explicit treatment of the stabilization also improves accuracy. The curves have the same slope in the explicit and implicit case, but the errors are approximately a factor three smaller and the time step differs by a factor of four. This shows that for the lowest-order time discretization, the explicit method is expected to be substantially cheaper than the fully implicit one if a specific accuracy has to be obtained. The situation is less clear for the second-order scheme where also the time step is taken four times smaller in the explicit case, but the resulting reduction in error is only a factor of two.

5.2. Flow around a cylinder at $Re = 10^2$

Here we consider the classical benchmark proposed in [27] and we refer to that work for details on the configuration. The problem consists in the computation of the flow around a cylinder at Reynolds 10^2, and the benchmark quantities that we consider are the drag C_D and the lift C_L on the cylinder. We compare the fractional-step projection scheme using implicit treatment of the velocity stabilization with the fully implicit monolithic scheme using either BDF1 or BDF2 for the time discretization. We have used three unstructured computational meshes with 2886, 11055 and 44540 vertices. Note that smaller time steps have been considered for the BDF1 schemes. The results are reported in Tables 1 and 2. As expected, the BDF2 scheme delivers comparable accuracy with larger time steps. We can also observe that the BDF1 projection scheme provides practically the same results as the BDF1 monolithic scheme for sufficiently small time steps.

TABLE 1. Computed drag and lift using the BDF2 monolithic solver.

		BDF2 monolithic	
NDOF	τ	C_D	C_L
3×2886	10^{-2}	3.34	1.12
3×11055	5×10^{-3}	3.27	1.05
3×44540	2.5×10^{-3}	3.24	1.03
	lower ref.	3.22	0.99
	upper ref.	3.24	1.01

TABLE 2. Comparison of the computed drag and lift using the BDF1 monolithic and fractional-step solvers.

		BDF1 monolithic		BDF1 fractional-step	
NDOF	τ	$C_{D_{\max}}$	$C_{L_{\max}}$	$C_{D_{\max}}$	$C_{L_{\max}}$
3×2886	5×10^{-3}	3.27	1.04	3.28	1.13
3×11055	2.5×10^{-3}	3.25	1.07	3.26	1.09
3×44540	$1.25 \cdot 10^{-3}$	3.24	1.05	3.24	1.06
	lower ref.	3.22	0.99	3.22	0.99
	upper ref.	3.24	1.01	3.24	1.01

5.3. Navier–Stokes mixing layer at $Re = 10^4$

Finally we propose a qualitative study of a Kelvin–Helmholtz shear layer. This test was proposed in [24] as a model problem for 2D turbulence and was shown to have the characteristic cubic decay of the power spectrum.
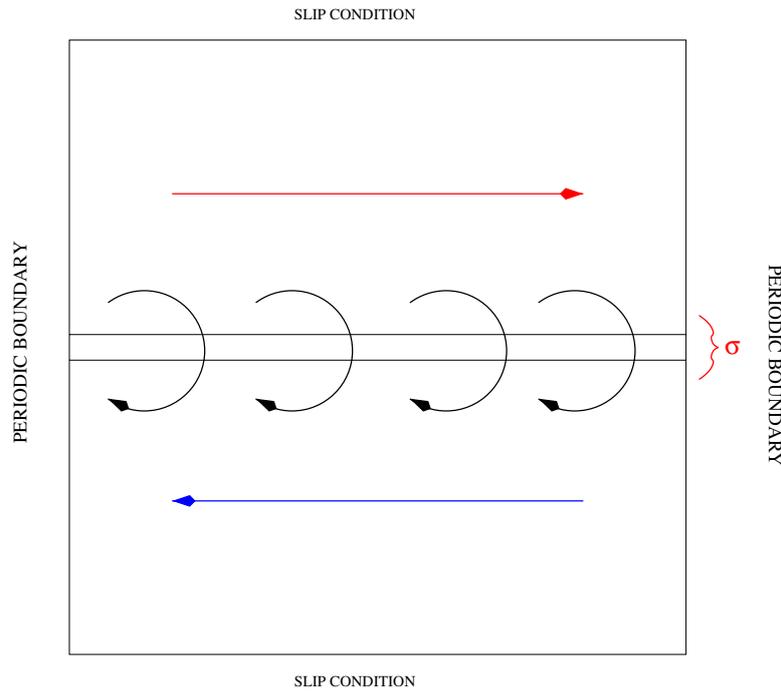
FIGURE 2. Computational configuration for the Kelvin–Helmholtz shear layer instability.

The problem has a smooth solution, but the Sobolev norm of the exact solution is large. In particular, the velocity gradient is large in the shear layer and the problem is known to be very sensitive to perturbations of initial data and numerical viscosity. For other numerical experiments on this test case see [3,16,21]. A schematic illustration of the problem setup is presented in Figure 2. The computational domain Ω is the unit square, $\boldsymbol{u}_\infty = 1$, $\beta_\Omega = \frac{1}{28}$, and the viscosity is set to $\nu = 3.571 \times 10^{-6}$. The objective is to explore whether the use of the second-order time discretization remains stable while delivering the expected improved accuracy and to study how the splitting affects the approximation accuracy. As reference solutions we use computations from a monolithic solver with continuous interior penalty stabilization taken from [3]. The time step is $\tau = 1.5625 \times 10^{-3}$ (as in [3]).

Figure 3 shows a comparison between the solutions obtained using the fractional-step method combined with either BDF1 (a) or BDF2 (b) on a mesh with 80×80 elements using piecewise affine approximation. We present a series of snapshots at the non-dimensional times $t = 80$, 120, 140. In Figure 3c we report the reference solution obtained using BDF2 time discretization and a monolithic solver using the same space discretization and at the same time levels. On this coarse scale, the two fractional-step solutions appear to be of similar quality. The two vortices are merging in the first snapshot at $t = 80$. The solution obtained using the monolithic solver on the other hand has not yet entered the transition phase in the first snapshot. A possible explanation of this is that the fractional-step method is more dissipative on coarse meshes, since it is known that excessive dissipation tends to speed up the transition sequence.

In Figure 4 we then consider the same sequence of snapshots on the finest mesh with 320×320 elements. In Figures 4a and 4b we present the snapshots of the fractional-step method using BDF1 and BDF2 respectively. Figures 4c and 4d report snapshots of solutions obtained using the monolithic solver on a 320×320 mesh and piecewise affine approximation (c) and on a 160×160 mesh and piecewise quadratic approximation (d). In this case, the improved detail of the fractional-step method using BDF2 compared to the one using BDF1 can be clearly seen. On this resolution the fractional-step solutions using BDF2 has similar qualitative behaviour as those obtained using the monolithic scheme with BDF2.
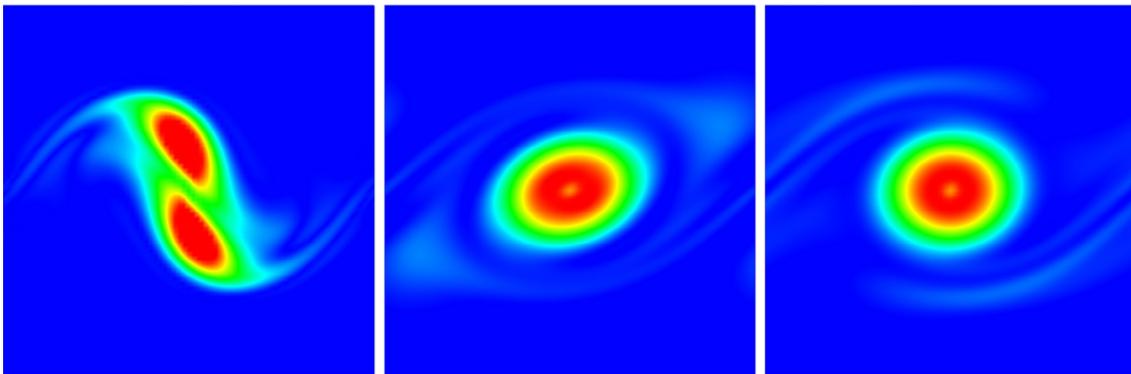
(a) Fractional-step BDF1, $k = 1$, 80×80 mesh
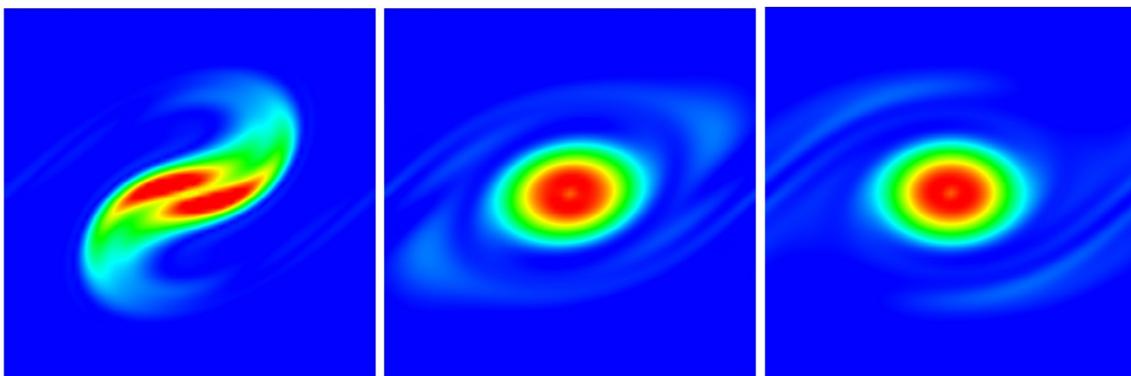
(b) Fractional-step BDF2, $k = 1$, 80×80 mesh
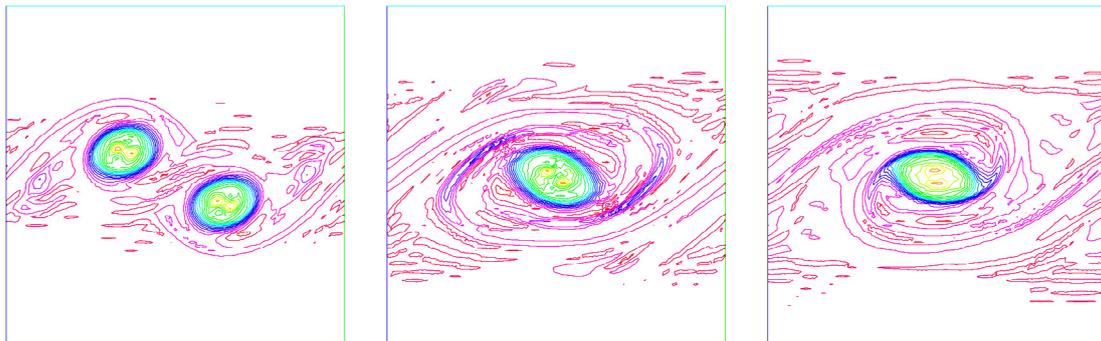
(c) Monolithic BDF2, , $k = 1$, 80×80 mesh

FIGURE 3. Comparison of fractional-step BDF1 (a), BDF2 (b), and monolithic BDF2 time scheme (c); time levels, from left to right, $t = 80, 120, 140$; computational mesh: 80×80; piecewise affine approximation.
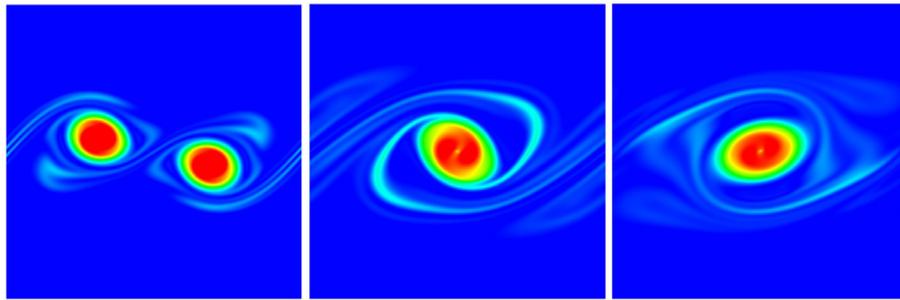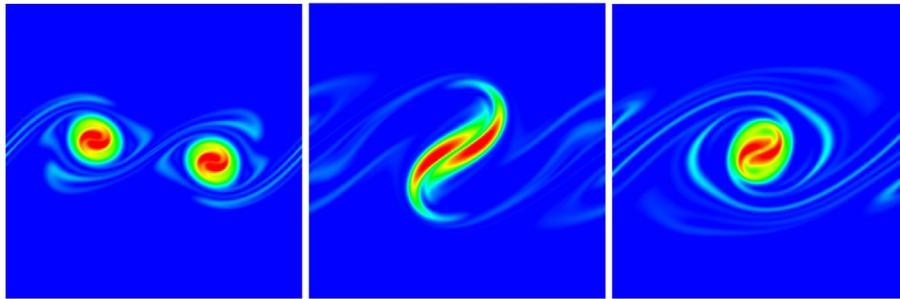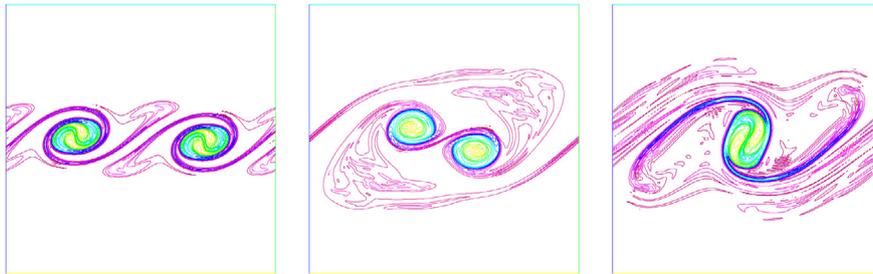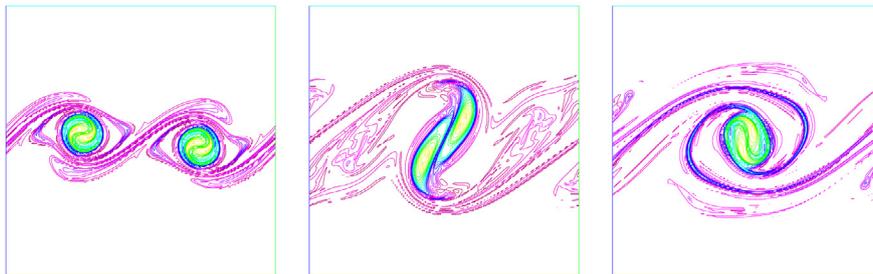
(a) Fractional-step BDF1, $k = 1$, 320×320 mesh

(b) Fractional-step BDF2, $k = 1$, 320×320 mesh

(c) Monolithic BDF2, $k = 1$, 320×320 mesh

(d) Monolithic BDF2, $k = 2$, 160×160 mesh

FIGURE 4. Comparison of fractional-step BDF1 (a), BDF2 (b); time levels, from left to right, $t = 80, 120, 140$; computational mesh: 320×320; piecewise affine approximation. Monolithic computations: BDF2; 320×320; piecewise affine approximation (c); BDF2; 160×160; piecewise quadratic approximation (d).

References

[1] R. Becker and M. Braack, A two-level stabilization scheme for the Navier–Stokes equations. In *Numerical Mathematics and Advanced Applications.* Springer, Berlin (2004) 123–130.

[2] M. Braack, E. Burman, V. John and G. Lube, Stabilized finite element methods for the generalized Oseen problem. *Comput. Methods Appl. Mech. Engrg.* **196** (2007) 853–866.

[3] E. Burman, Interior penalty variational multiscale method for the incompressible Navier–Stokes equation: monitoring artificial dissipation. *Comput. Methods Appl. Mech. Engrg.* **196** (2007) 4045–4058.

[4] E. Burman and M.A. Fernández, Continuous interior penalty finite element method for the time-dependent Navier–Stokes equations: space discretization and convergence. *Numer. Math.* **107** (2007) 39–77.

[5] E. Burman and M.A. Fernández, Galerkin finite element methods with symmetric pressure stabilization for the transient Stokes equations: stability and convergence analysis. *SIAM J. Numer. Anal.* **47** (2008/09) 409–439.

[6] E. Burman and P. Hansbo, Edge stabilization for Galerkin approximations of convection-diffusion-reaction problems. *Comput. Methods Appl. Mech. Engrg.* **193** (2004) 1437–1453.

[7] E. Burman, M.A. Fernández and P. Hansbo, Continuous interior penalty finite element method for Oseen's equations. *SIAM J. Numer. Anal.* **44** (2006) 1248–1274.

[8] T. Chacón Rebollo, M. Gómez Mármol and M. Restelli, Numerical analysis of penalty stabilized finite element discretizations of evolution Navier–Stokes equations. *J. Sci. Comput.* **63** (2015) 885–912.

[9] R. Codina, Stabilization of incompressibility and convection through orthogonal sub-scales in finite element methods. *Comput. Methods Appl. Mech. Engrg.* **190** (2000) 1579–1599.

[10] R. Codina and S. Badia, On some pressure segregation methods of fractional-step type for the finite element approximation of incompressible flow problems. *Comput. Methods Appl. Mech. Engrg.* **195** (2006) 2900–2918.

[11] D.A. Di Pietro and A. Ern, Discrete functional analysis tools for discontinuous Galerkin methods with application to the incompressible Navier–Stokes equations. *Math. Comp.* **79** (2010) 1303–1330.

[12] D.A. Di Pietro and A. Ern, Mathematical Aspects of Discontinuous Galerkin Methods. Vol. 69 of *Math. Appl.* Springer-Verlag, Berlin (2012).

[13] A. Ern and J.-L. Guermond, Discontinuous Galerkin methods for Friedrichs' systems. I. General theory. *SIAM J. Numer. Anal.* **44** (2006) 753–778.

[14] A. Ern and J.-L. Guermond, Weighting the edge stabilization. *SIAM J. Numer. Anal.* **51** (2013) 1655–1677.

[15] V. Girault, B. Rivière and M.F. Wheeler, A discontinuous Galerkin method with nonoverlapping domain decomposition for the Stokes and Navier–Stokes problems. *Math. Comput.* **74** (2005) 53–84.

[16] V. Gravemeier, W.A. Wall and E. Ramm, Large eddy simulation of turbulent incompressible flows by a three-level finite element method. *Int. J. Numer. Methods Fluids* **48** (2005) 1067–1099.

[17] J.-L. Guermond, Stabilization of Galerkin approximations of transport equations by subgrid modeling. *ESAIM: M2AN* **33** (1999) 1293–1316.

[18] J.-L. Guermond and L. Quartapelle, On the approximation of the unsteady Navier–Stokes equations by finite element projection methods. *Numer. Math.* **80** (1998) 207–238.

[19] J.-L. Guermond, A. Marra and L. Quartapelle, Subgrid stabilized projection method for 2D unsteady flows at high Reynolds numbers. *Comput. Methods Appl. Mech. Engrg.* **195** (2006) 5857–5876.

[20] J.L. Guermond, P. Minev and Jie Shen. An overview of projection methods for incompressible flows. *Comput. Methods Appl. Mech. Engrg.* **195** (2006) 6011–6045.

[21] V. John, An assessment of two models for the subgrid scale tensor in the rational LES model. *J. Comput. Appl. Math.* **173** (2005) 57–80.

[22] C. Johnson and J. Pitkäranta, An analysis of the discontinuous Galerkin method for a scalar hyperbolic equation. *Math. Comput.* **46** (1986) 1–26.

[23] C. Johnson, U. Nävert and J. Pitkäranta, Finite element methods for linear hyperbolic problems. *Comput. Methods Appl. Mech. Engrg.* **45** (1984) 285–312.

[24] M. Lesieur, C. Staquet, P. Le Roy and P. Comte, The mixing layer and its coherence examined from the point of view of two-dimensional turbulence. *J. Fluid Mech.* **192** (1988) 511–534.

[25] J. Nitsche, Über ein Variationsprinzip zur Lösung von Dirichlet-Problemen bei Verwendung von Teilräumen, die keinen Randbedingungen unterworfen sind. Collection of articles dedicated to Lothar Collatz on his sixtieth birthday. *Abh. Math. Sem. Univ. Hamburg* **36** (1971) 9–15.

[26] A. Prohl, Projection and quasi-compressibility methods for solving the incompressible Navier–Stokes equations. *Advances in Numerical Mathematics.* B. G. Teubner, Stuttgart (1997).

[27] S. Turek and M. Schäfer, Benchmark computations of laminar flow around cylinder. Flow Simulation with High-Performance Computers II. Vieweg (1996).